1-1-1998

Context-dependent protein stabilization by methionine-to-leucine substitution shown in T4 lysozyme

Leigh Ann Lipscomb
University of Oregon

Nadine C. Gassner
University of Oregon

Sheila D. Snow
University of Oregon

Aimee M. Eldridge
University of Oregon

Walter A. Baase
University of Oregon

See next page for additional authors

Authors

Leigh Ann Lipscomb, Nadine C. Gassner, Sheila D. Snow, Aimee M. Eldridge, Walter A. Baase, Devin L. Drew, and Brian W. Matthews

Protein Science (1998), 7:765–773. Cambridge University Press. Printed in the USA.

Context-dependent protein stabilization by methionine-to-leucine substitution shown in T4 lysozyme

LEIGH ANN LIPSCOMB,[1] NADINE C. GASSNER, SHEILA D. SNOW,[2]
AIMEE M. ELDRIDGE, WALTER A. BAASE, DEVIN L. DREW, AND BRIAN W. MATTHEWS

Institute of Molecular Biology, Howard Hughes Medical Institute and Departments of Chemistry and Physics, University of Oregon, Eugene, Oregon 97403

(RECEIVED September 30, 1997; ACCEPTED December 15, 1997)

Abstract

The substitution of methionines with leucines within the interior of a protein is expected to increase stability both because of a more favorable solvent transfer term as well as the reduced entropic cost of holding a leucine side chain in a defined position. Together, these two terms are expected to contribute about 1.4 kcal/mol to protein stability for each Met → Leu substitution when fully buried. At the same time, this expected beneficial effect may be offset by steric factors due to differences in the shape of leucine and methionine. To investigate the interplay between these factors, all methionines in T4 lysozyme except at the amino-terminus were individually replaced with leucine. Of these mutants, M106L and M120L have stabilities 0.5 kcal/mol higher than wild-type T4 lysozyme, while M6L is significantly destabilized (−2.8 kcal/mol). M102L, described previously, is also destabilized (−0.9 kcal/mol). Based on this limited sample it appears that methionine-to-leucine substitutions can increase protein stability but only in a situation where the methionine side chain is fully or partially buried, yet allows the introduction of the leucine without concomitant steric interference. The variants, together with methionine-to-lysine substitutions at the same sites, follow the general pattern that substitutions at rigid, internal sites tend to be most destabilizing, whereas replacements at more solvent-exposed sites are better tolerated.

Keywords: hydrophobic effect; methionine; protein design; protein stabilization; side-chain entropy; T4 lysozyme

The rationale for this study is to determine whether, and to what degree, methionine-to-leucine substitutions are useful as a general method to increase protein stability. The van der Waals volume occupied by leucine is the same as for methionine (Creighton, 1992). Both side chains are non-polar, although the solvent transfer free energy for leucine is about 0.6 kcal/mol greater than that for methionine (Fauchére & Pliska, 1983). Also, a buried methionine has one more bond than leucine that is immobilized on folding, incurring a greater entropy cost upon immobilization within a folded protein. Ignoring possible steric and other effects, the above two terms correspond to an estimated loss of stability of about 1.4 kcal/mol for each leucine-to-methionine substitution at a buried site within a folded protein (Gassner et al., 1996). Consistent with this expectation, a series of six leucine-to-methionine replacements within the core of T4 lysozyme destabilized the protein by 0.4 to 1.9 kcal/mol (Gassner et al., 1996).

If leucine-to-methionine replacements within the core consistently destabilize a protein, one can ask whether the inverse substitutions might increase stability. The key question is whether leucine side chains can be readily accommodated at methionine sites or whether there will be steric interference that will offset the expected benefit of the enhanced transfer free energy and reduced entropic cost outlined above. It was previously shown, for example, that a methionine-to-phenylalanine substitution stabilized subtilisin BPN (Pantoliano et al., 1989) but the Met-to-Leu replacement at site 102 in T4 lysozyme was somewhat destabilizing (Hurley et al., 1992). A Met-to-Leu replacement in *Staphylococcal nuclease* was predicted to increase stability by 1.6 kcal/mol (Yamaotsu et al., 1993) but actually decreased stability by 0.8 kcal/mol (Spencer & Stites, 1996). In a somewhat different context Estell et al. (1985) replaced Met 222 of subtilisin with various amino acids to increase resistance to chemical oxidation.

Reprint requests to: Brian W. Matthews, Institute of Molecular Biology, University of Oregon, Eugene, Oregon 97403; e-mail: brian@uoxray.uoregon.edu.

[1]Present address: Department of Biochemistry and Molecular Biology, University of Georgia, Athens, Georgia 30602.

[2]Present address: Dow Neurological Sciences Institute, 1120 NW 20th, Portland, Oregon 97209.

Table 1. *Solvent accessibility of methionines in T4 lysozyme*[a]

Amino acid	Fractional accessibility to solvent	
	Main chain	Side chain
Met 1	0.61	0.14
Met 6	0.00	0.00
Met 102	0.00	0.02
Met 106	0.63	0.22
Met 120	0.00	0.21

[a]Solvent accessibilities were estimated as in Alber et al. (1987).

Cysteine-free pseudo-wild-type lysozyme (WT*) has five methionines. Their accessibility to solvent, based on the pseudo-wild-type crystal structure (Eriksson et al., 1993) is summarized in Table 1. To determine the effect of methionine substitution on stability and structure we made a set of representative replacements. First, leucine was substituted in turn for Met 6, Met 106, and Met 120. Met 102 has previously been replaced with leucine by Hurley et al. (1992). As examples of less conservative substitutions, Met 106 and Met 120 were replaced with lysine. The Met 102 → Lys mutant has previously been described by Dao-pin et al. (1991). The fifth methionine (Table 1) corresponds to the initiator codon and was not replaced.

Results

The five mutant lysozymes described here, M6L, M106L, M120L, M120K, and M106K were purified by standard procedures (Poteete et al., 1991). Thermodynamic data are given in Table 2 and activities in Table 3. Each of the variants could be crystallized leading to the structural results reviewed below. The coordinates have been deposited in the Brookhaven Data Bank for immediate release (ID codes 230L-234L).

Table 2. *Stability of mutant lysozymes*[a]

Variant	ΔT_m (°C)	ΔH (kcal/mol)	$\Delta\Delta G$ (kcal/mol)
Methionine-to-leucine			
M6L	−10.6	61	−2.8
M102L[b]	−2.4	96	−0.9
M106L	1.7	111	0.5
M120L	1.7	116	0.5
Methionine-to-lysine			
M102K[c]	−35	12	−9
M106K	−10.5	90	−3.4
M120K	−4.8	99	−1.6

[a]Stability measurements were at pH 3.0 as described in the text. ΔT_m is the change in melting temperature relative to WT* lysozyme. ΔH is the enthalpy of unfolding measured at the T_m of the mutant. $\Delta\Delta G$ is the change in free energy of unfolding of the mutant relative to WT* so that a positive $\Delta\Delta G$ indicates a mutant of enhanced thermostability.
[b]Hurley et al. (1992).
[c]Dao-pin et al. (1991).

Table 3. *Activities of mutant lysozymes*[a]

Mutant	Activity relative to wild type (%)
M6L	94
M102L	75
M106L	103
M120L	104
M102K	42
M106K	4
M120K	74

[a]Activities were measured as described in the text.

Methionine 6 → leucine

Met 6 is located in the center of T4 lysozyme, between the N- and C-terminal lobes, and is completely buried (Table 1).

Of the methionine-to-leucine mutants described here, Met 6 → Leu (M6L) has the largest structural perturbations. Globally, the X-ray structure is similar to WT*, but there are a number of structural differences surrounding residue 6. The substituted leucine side chain does not assume the extended conformation of the WT* methionine (Fig. 1). Rather, it adopts a different rotamer, resulting in formation of a 40 $Å^3$ cavity not present in the WT* structure. To avoid a steric clash, the side chain of Trp 158 moves roughly 0.4 Å from its WT* position. The side chain of Tyr 161 moves roughly 0.2 Å toward the cavity, presumably to decrease its size.

The structure of M6L has many similarities to the previously determined structure of M6I (Faber & Matthews, 1990). Both structures have cavities proximal to the site of mutation of about 40 $Å^3$, and both are destabilized equally relative to WT*. Both mutants crystallized in space groups isomorphous ($P3_221$) and also non-isomorphous ($P2_12_12_1$) with WT*.

Methionine 106 → leucine

With the exception of residue 1, residue 106 is the most solvent-exposed methionine of T4 lysozyme. In general, the structure of M106L is very similar to WT*, although the leucine side chain assumes a rotamer different from WT* methionine (Fig. 2). In contrast to M6L, there are only small adjustments in the surrounding residues, suggesting that introduction of the leucine side chain does not result in steric interference with neighboring protein atoms or in the formation of cavities. The Leu 106 side chain is actually better ordered in the mutant structure (crystallographic *B*-factor of 16.0 $Å^2$) than is Met 106 in the WT* structure (*B*-factor of 39.1 $Å^2$) (Table 4).

Methionine 120 → leucine

The methionine at residue 120 is partially solvent exposed (Table 1). The super-imposition of M120L and WT* (Fig. 3) shows striking similarity between the two structures, including the mutated amino acid. The C^α, C^β, C^γ, and $C^{\delta 1}$ atoms of the leucine side chain all virtually super-impose on their counterparts in the methionine. The $C^{\delta 2}$ atom extends toward the Arg 119 side chain, occupying a space vacant in WT*. The lack of any significant perturbation indicates that the introduced leucine causes little if

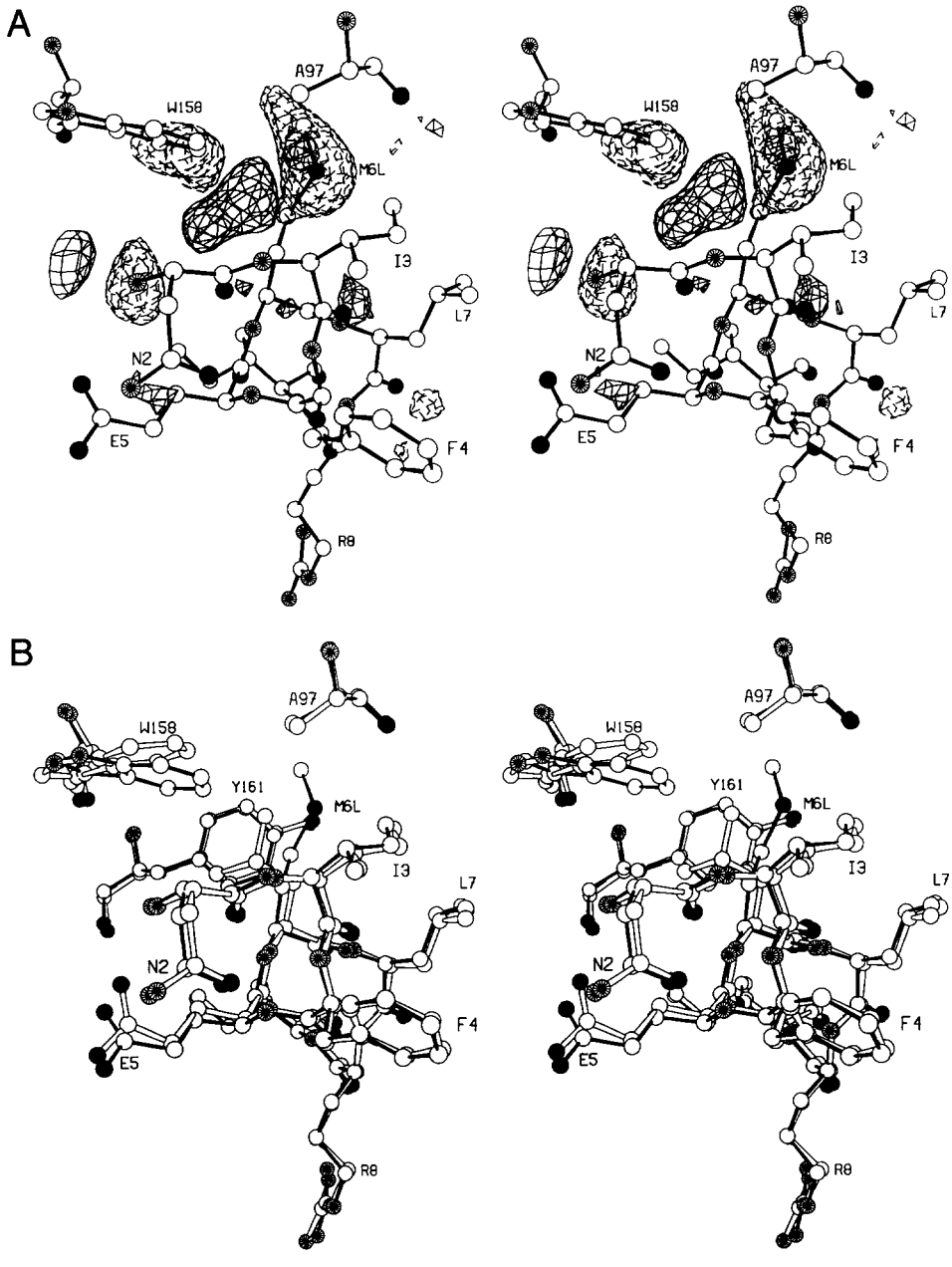

Fig. 1. A: Map showing the difference in electron density between M6L and WT* lysozyme. Coefficients are ($F_{mut} - F_{WT*}$), where F_{mut} and F_{WT*} are the observed structure amplitudes for the mutant and WT* structures. Phases are from the refined structure of WT*. The map is contoured at $+3\sigma$ (solid lines) and -3σ (broken lines), where σ is the RMS density throughout the unit cell. The super-imposed structure is of WT* with oxygen and sulfur atoms drawn solid, nitrogen atoms with spokes and carbon atoms open. **B:** Super-position of the structure of M6L (open bonds) on WT* (solid bonds).

any steric hindrance. As with site 106, the introduced Leu 120 side chain is better ordered than Met 120 in WT* (Table 4).

Methionine 106 → lysine

The global conformation of M106K is similar to WT*, although there are differences in the conformation of the substituted residue (Fig. 4). The N^{ζ} of Lys 120 points in a direction roughly 180° from C^{ϵ} of the WT* methionine. Lys 120 is enclosed in a largely hydrophobic environment between Trp 138 and Phe 114. In the observed structure N^{ζ} approaches the Phe 114 side chain within 3.4 Å. In alternate conformations, the lysine would approach Trp 138. The lysine is somewhat disordered (Table 4), with the three most-distal side-chain atoms having crystallographic *B*-factors above 69 Å^2.

Methionine 120 → lysine

The distal side-chain atoms of Met 120 are partially exposed to solvent, allowing easy access of the introduced lysine to the

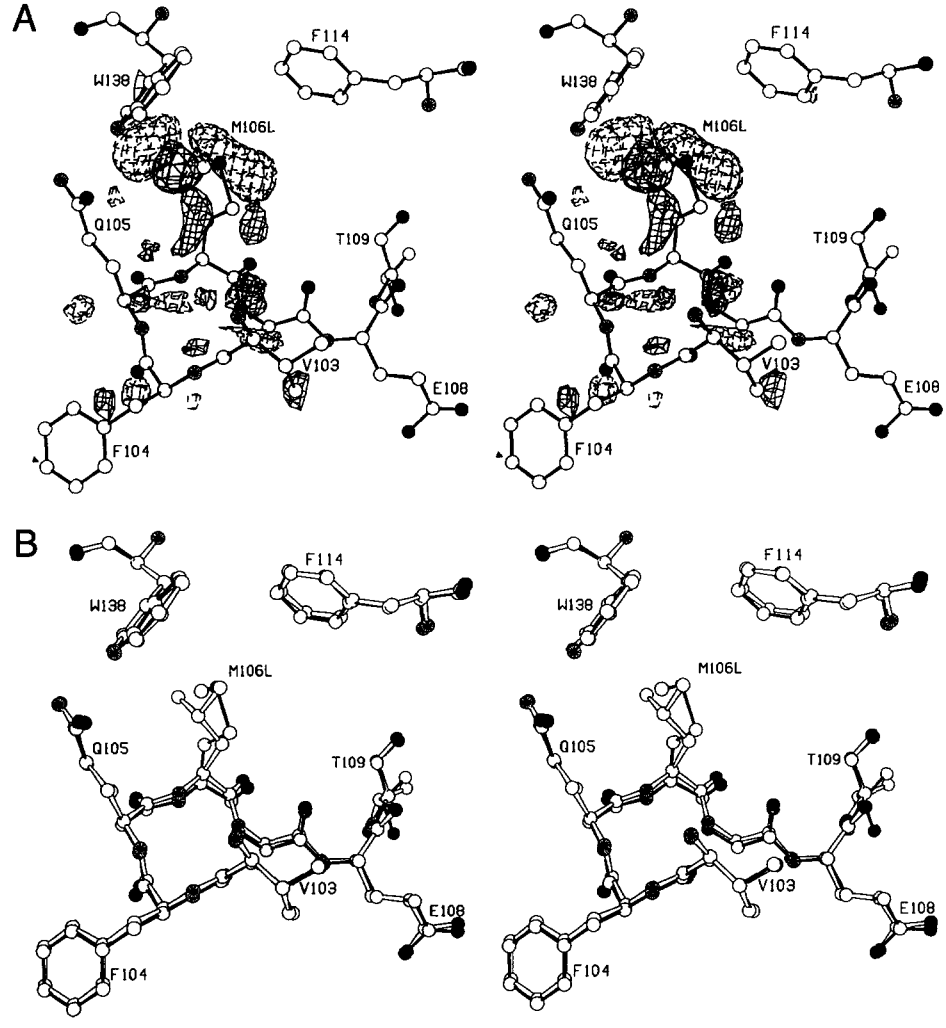

Fig. 2. A: Difference map for mutant M106L super-imposed on the structure of WT* lysozyme. All procedures and conventions as in Figure 1A. **B:** Super-position of the structure of M106L (open bonds) on WT* lysozyme (solid bonds).

aqueous milieu. The structure of M120K is generally similar to WT*, with a slight difference in side-chain location at the mutation site (Fig. 5). The side chain crystallographic *B*-factors of the introduced lysine increase with distance from the α-carbon backbone, and exceed 58 Å^2 for the atoms beyond C$^\gamma$ (Table 4).

Table 4. *Crystallographic B-factors of substituted residues*[a]

	B-factors			*B*-factors			*B*-factors	
Amino acid in WT*	Main chain (Å^2)	Side chain (Å^2)	Amino acid in mutant	Main chain (Å^2)	Side chain (Å^2)	Amino acid in mutant	Main chain (Å^2)	Side chain (Å^2)
Met 6	16.6	10.8	Leu 6	10.7	18.9	—		
Met 102	17.2	18.8	Leu 102[b]	18.2	21.2	Lys 102[c]	19.0	44.3
Met 106	23.6	39.1	Leu 106	14.7	16.0	Lys 106	32.1	67.3
Met 120	20.0	25.2	Leu 120	11.3	10.8	Lys 120	14.7	56.3

[a]The value quoted for the mainchain is the average of the crystallographic *B*-factors for O, N, C, and C$^\alpha$; that for the side chain includes C$^\beta$ and all distal atoms.
[b]Hurley et al. (1992).
[c]Dao-pin et al. (1991).

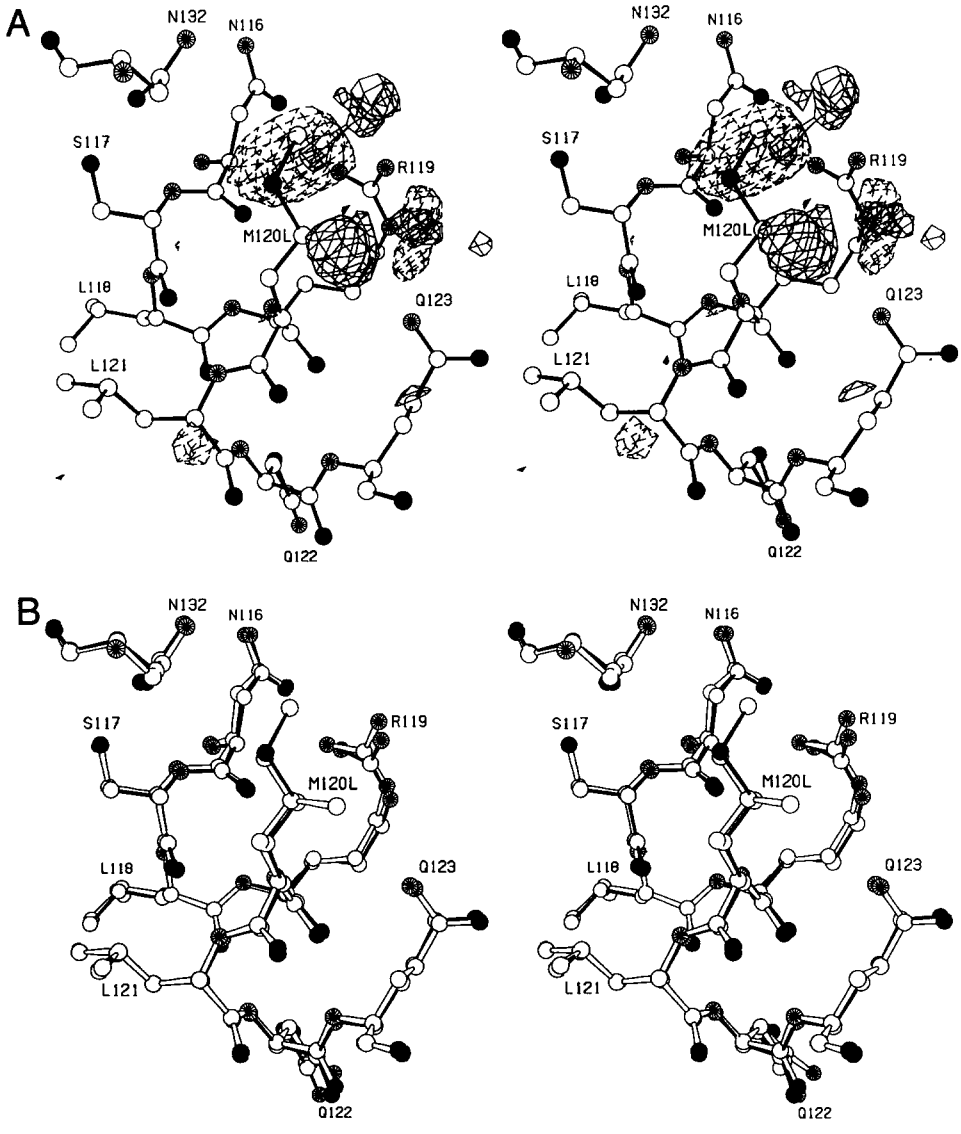

Fig. 3. A: Difference map for mutant M120L super-imposed on the structure of WT* lysozyme. All procedures and conventions as in Figure 1A. **B:** Super-position of the structure of M120L (open bonds) on WT* lysozyme (solid bonds).

Discussion

There is extensive evidence that substitutions at solvent-accessible sites on the surface of proteins tend to cause small changes in stability, whereas substitutions at internal sites can be much more influential (Alber et al., 1987; Matthews, 1993). The present substitutions follow the same trend. Met 102 is completely buried, and substitution with lysine is very destabilizing, especially at pH values where the lysine is likely to be protonated (Table 2; Dao-pin et al., 1991). The side chains of Met 106 and 120 are at least partly exposed to solvent (Table 1) and lysine substitutions at these sites are better tolerated (Table 2). The methionine-to-leucine substitutions follow a similar pattern. Replacements at the buried Met 6 and Met 102 sites are destabilizing, while replacements at the partly solvent-exposed sites actually increase stability slightly (Table 2).

With the notable exception of M106K, each of the variants constructed here has activity within about a factor of two equal to that of WT*. In an adduct of T4 lysozyme with an extended peptidoglycan cell-wall fragment, the side chain of Met 106 makes van der Waals contacts with the peptidic part of the fragment (Kuroki et al., 1993). In the structure of M106K (Fig. 4B) the ϵ-amino group of Lys 106 occupies a position that would potentially interfere with bound substrate. Possible steric interference was checked by super-imposing the structure of M106K on the lysozyme–peptidoglycan complex described by Kuroki et al. (1993). In this super-position there are five steric clashes (2.1–2.8 Å) between either C^{ϵ} or N^{ζ} of Lys 106 and the L-Ala-D-Glu portion of the peptidoglycan. Because of the length of the lysine side chain it was not possible to move C^{ϵ} and N^{ζ} into a sterically acceptable position. When the structure of M106L was super-imposed on the lysozyme–peptidoglycan complex there were three close approaches in the range of 2.3–2.8 Å, all involving $C^{\delta 2}$ of Leu 106. In contrast to Lys 106, however, these close approaches could readily be alleviated (increased to at least 3.2 Å) by small adjustments ($\leq 20°$) in the χ_1 and χ_2 angles of Leu 106. The apparent steric interfer-

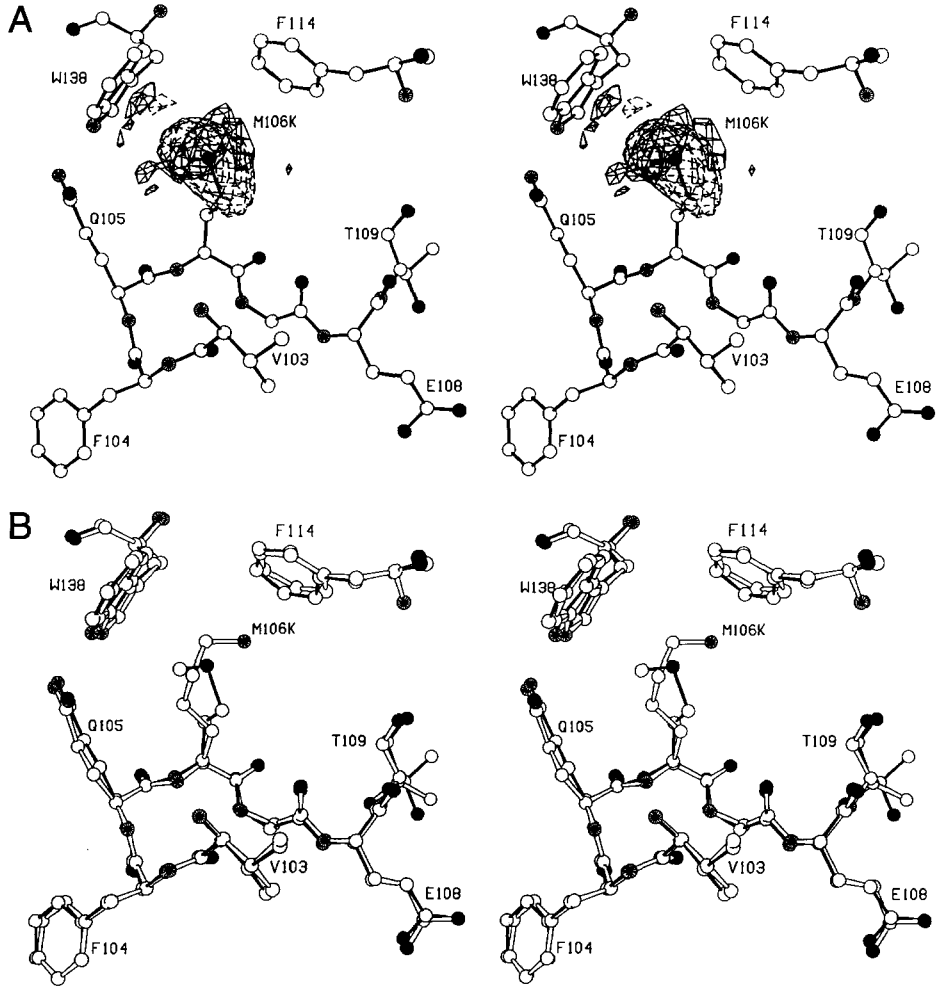

Fig. 4. A: Difference map for mutant M106K super-imposed on the structure of WT* lysozyme. All procedures and conventions as in Figure 1A. **B:** Super-position of the structure of M106K (open bonds) on WT* lysozyme (solid bonds).

ence between M106K and bound substrate could explain the reduction in activity for this mutant.

The destabilization associated with each of the methionine-to-lysine substitutions reflects their different environments. Met 102 is fully buried within the hydrophobic core of the protein, and it is no surprise that its replacement with lysine is very deleterious (Dao-pin et al., 1991). Indeed, this is the most destabilizing point mutant of T4 lysozyme that has been characterized to date. The side chains of Met 106 and Met 120 are both about 80% buried (Table 1), but this is somewhat deceptive. Met 106 contributes to the hydrophobic core of the protein and has as neighbors Met 102, Phe 114, and Trp 138. In contrast, Met 120 extends toward the outside of the protein and is surrounded by Asn 116, Arg 119, Arg 125, and Asn 132. The introduction of a lysine is better tolerated in the context of the more polar environment of site 120 than in the less polar environment of site 106. In the mutant structures M102K, M106K, and M120K the solvent-accessible surface areas of the ϵ-amino groups of the introduced lysines (i.e., Lys 102, Lys 106, and Lys 120) are, respectively, 0 $Å^2$, 15 $Å^2$, and 25 $Å^2$. This can be compared with the average value of 36 $Å^2$ for all lysines in the WT* structure. Thus, as the ϵ-amino group becomes more buried, there is a progressive loss in stability (Table 2).

The thermodynamic and structural characteristics outlined above make it possible to address the key question asked in the present work, namely whether methionine-to-leucine substitutions can be used to increase protein stability. As shown in Table 2, two of the substitutions, Met 106 $\rightarrow$ Leu and Met 120 $\rightarrow$ Leu do increase stability, albeit modestly. The other two mutants, M6L and M102L, however, are significantly destabilized.

Can one predict ahead of time those substitutions that are likely to be beneficial and those that are not. The available structural and thermodynamic data do give some encouragement.

As one progresses from the least stable variant (M6L) to the most stable ones (M106L and M120L), there is a corresponding change in the structural response to the substitution. In the case of M6L, the introduction of the leucine causes substantial movement in several nearby residues (Fig. 1B). Also, the leucine adopts a conformation very different from the methionine that it replaces, resulting in a cavity of 40 $Å^3$. These rearrangements are indicative of significant steric interference between the introduced leucine and the atoms defining the space that it has to accommodate it.

In the case of M102L, which is destabilized but not as much as M6L, the substituted leucine again adopts a conformation very different from the methionine that it replaces, but the changes in

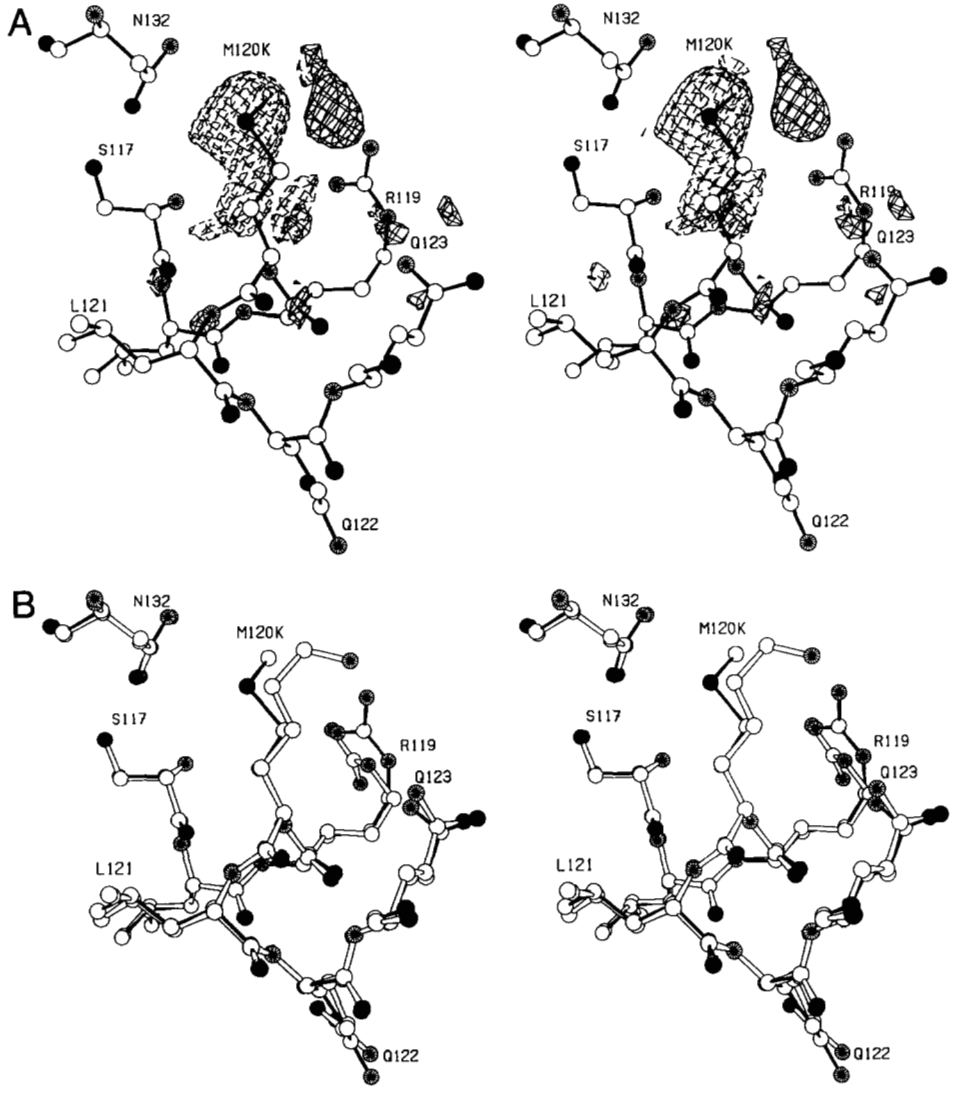

Fig. 5. A: Difference map for mutant M120K super-imposed on the structure of WT* lysozyme. All procedures and conventions as in Figure 1A. **B:** Super-position of the structure of M120K (open bonds) on WT* lysozyme (solid bonds).

the surrounding protein atoms are much more modest (Hurley et al., 1992).

Proceeding upward in stability to M106L, the substituted side chain has a conformation different from its parent, but the surrounding atoms hardly move at all (Fig. 2B). In contrast to the destabilized mutants, M6L and M102L, leucine can be introduced with little, if any, steric hindrance from the rest of the protein. Similarly to M106L, it appears that a leucine can be introduced at site 120 with little, if any, steric interference (Fig. 3B).

In cases such as M106L and M120L, one can begin to realize some of the expected stabilization from methionine-to-leucine substitutions. In neither case, however, does the increase in stability approach the theoretically expected value of about 1.4 kcal/mol. For both M106L and M120L this is due at least in part to the fact that their side chains are partially exposed to solvent (Table 1) and do not realize their full solvent transfer potential. It may also be that there is some residual strain introduced by the substitution.

For both M6L and M102L, the introduced leucine side chains have higher crystallographic *B*-factors than the methionines that they replace (Table 4). This suggests that these leucines do not pack as well. In contrast, for both M106L and M120L the introduced leucines have lower side chain *B*-factors than methionines at the same sites (Table 4). In these two cases, in which the protein as a whole is stabilized, the packing appears to be improved in the mutants.

Because the present work suggests that methionine-to-leucine substitutions are, at best, of modest value in increasing protein stability, and may be deleterious, we carried out a simple model-building experiment to try to assess the likely outcome of a given substitution. Starting with the coordinates of WT* lysozyme, we attempted to model build a leucine side chain at each substitution site. In each case the side chain was adjusted so as to minimize steric clashes with surrounding atoms, using side-chain rotamer angles that were within ±15° of the staggered conformation. The results are summarized in Table 5. As can be seen, for both Leu 6 and Leu 102 the $C^{\delta 1}$ and $C^{\delta 2}$ atoms have prohibitively short approaches to neighboring atoms. These are the two mutants that are destabilized relative to WT*. In the case of Leu 106 and Leu 120,

Table 5. *Contacts between introduced leucine side chains and surrounding atoms based on model building*[a]

Model-built side chain		Contact atom in	Distance
Residue	Atom	WT* lysozyme	(Å)
Leu 6	$C^{\delta 1}$	Tyr 161 C $^{\delta}$	3.0
	$C^{\delta 1}$	Tyr 161 $C^{\delta 1}$	2.9
	$C^{\delta 2}$	Tyr 161 $C^{\delta 1}$	2.8
Leu 102	$C^{\delta 2}$	Ala 98 O	2.6
	$C^{\delta 1}$	Val 149 $C^{\delta 1}$	2.7
Leu 106	$C^{\delta 1}$	Val 111 N	2.8
	$C^{\delta 1}$	Val 111 $C^{\delta 2}$	2.3
Leu 120	None	None	—

[a]The table shows all interatomic approaches less than 3.0 Å between the model-built leucine side chain and the surrounding atoms in the model of WT* lysozyme.

the contacts, if any, are restricted to a single methyl of the leucine. These are the two variants that have stabilities greater than WT*. Thus, it would seem that rather straightforward model building, based on the parent structure, can give a good indication as to whether a methionine-to-leucine replacement at a given site is likely to increase protein stability.

Materials and methods

Mutagenesis, protein over-expression, and purification

The method of Kunkel et al. (1987) was used to prepare mutants in cysteine-free (C54T, C97A) pseudo-wild-type (WT*) lysozyme (Matsumura & Matthews, 1989). Mutants were cloned into the PHS1403 vector and transformed into *E. coli* RR1 cells. The double-stranded DNA sequence (Owen et al., 1983) was confirmed by automated methods incorporating polymerase chain reaction techniques (Perkin-Elmer ABI PRISM 377 DNA sequencer).

The mutant lysozymes were purified according to standard methods (Alber & Matthews, 1987; Muchmore et al., 1989; Poteete et al., 1991). The buffer used for crystal storage and data collection contained 0.1 M sodium phosphate pH 6.5, 0.55 M NaCl, and 0.02% NaN_3.

Measurement of activity

Activity of mutant proteins was assessed by using circular dichroism at 223 nm to follow the degradation of peptidoglycan fragments (Zhang et al., 1995; Gassner et al., 1997). Procedures were as described by Gassner et al. (1997) except that cell-wall fragments sufficient to produce a post-reaction signal of −55 millidegrees rather than −30 millidegrees at 223 nm were used.

Crystallization and structure determination

Crystals of M6L, M106K, M106L, M120L, and M120K were obtained at 4 °C by the hanging drop method under conditions similar to those used for crystallization of WT* and other T4 lysozyme mutants (Eriksson et al., 1993). Concentrated protein solutions (described above) were mixed 1:1 with precipitant solutions roughly 50 mM oxidized β-mercaptoethanol, 50 mM reduced β-mercaptoethanol, 1.8–2.0 M sodium/potassium phosphate, pH 6.5–7.1 (M102L, pH 6.5; M106K, pH 6.9; M6L, M120K and M106L, pH 7.1). The 1:1 mixture of protein and precipitant was equilibrated versus precipitant solution. Within two days to two weeks, crystals appeared that belonged to space group $P3_221$ and were isomorphous with those of WT* T4 lysozyme. Similarly to M6I (Faber & Matthews, 1990), a second crystal form was obtained for M6L (space group $P2_12_12_1$).

X-ray diffraction data were collected using a San Diego Multiwire Systems area detector in the ω scan mode (Hamlin, 1985). Difference density maps were calculated using structure factor amplitudes from WT* and the mutant, and WT* phases (Figs. 1–5). For each mutant, the maps had a prominent negative feature confirming the loss of the methionine sulfur atom (Figs. 1A–5A). Refinement of atomic coordinates was via standard protocols with TNT (Tronrud et al., 1987). Starting models for refinement were M6I in the $P3_221$ space group for M6L (Faber & Matthews, 1990), and WT* (Eriksson et al., 1993) for the other four mutants. Water and other solvent molecules were not included in the starting model. In the first stages of refinement interatomic distances and *B*-factors of the starting model were held constant to position the protein in the unit cell (rigid-body refinement). This was followed by rigid-body refinement of the two separate domains of the protein using X-ray data to 3.0 Å resolution. Positional and *B*-factor refinement was started with 3 Å resolution data and gradually increased (0.5 Å shells) to include the highest resolution data collected for the particular mutant. Putative solvent molecules were located using the PEKPIK utility of TNT. Those that met the following criteria were added to the model: (1) clear density in an Fo-Fc map, (2) hydro-

Table 6. *X-ray data collection and refinement statistics*[a]

	M6L	M106L	M120L	M106K	M120K
Resolution (Å)	1.9	1.9	1.9	2.5	1.7
Completeness (%)	80.1	77.0	82.0	95.6	71.5
R_{merge} (%)	7.7	7.5	6.5	6.7	4.6
R_c (%)	18.4	17.1	16.8	17.7	17.3
Bond discrepancy (Å)	0.016	0.010	0.015	0.018	0.017
Angle discrepancy (°)	2.3	2.5	2.4	2.7	2.4

[a]R_{merge} gives the agreement between repeated intensity measurements. R_c is the crystallographic residual for the refined model. The bond and angle discrepancies give the average deviation of the bonds and angles in the refined models from "ideal" stereochemistry.

gen bonding interaction(s) with either the protein or other solvent molecules, and (3) no violation of van der Waal's contacts. The addition of solvent molecules to the model was followed by positional and *B*-factor refinement. This cycle was continued until inspection of $2F_o - F_c$ and $F_o - F_c$ maps indicated that no additional solvent molecules should be included. The final model does not include solvent with *B*-factors higher than 80 Å^2. Data collection and refinement statistics are given in Table 6. The program EDPDB (Zhang & Matthews, 1995) was used to perform coordinate super-positions and to calculate solvent accessibility using a 1.4 Å radius probe. The program MS (Connolly, 1983) was used to perform cavity volume calculations using a 1.2 Å radius probe and the atomic van der Waals radii set from Eriksson et al. (1992).

Thermal stabilities

Thermal data were taken in 25 mM potassium chloride, 3 mM phosphoric acid, 17 mM monopotassium phosphate, pH 3. Variations in the fraction of folded protein were determined from the change in the circular dichroism (CD) at 223 nm with temperature (Eriksson et al., 1993). Application of a two-state van't Hoff analysis gave a T_m of 51.7 °C and a ΔH at the T_m of 114 kcal/mol for WT* in this buffer (see Zhang et al., 1995). Random error estimates for ΔT_m are ± 0.2 °C and for ΔH are ±5 kcal/mol. $\Delta\Delta G$ values were calculated using a constant ΔC_p model (with ΔC_p equal to 1.8 kcal/mol) at an isotherm of 47 °C. Errors for $\Delta\Delta G$ are estimated to be ±0.14 kcal/mol for small values of $\Delta\Delta G$ increasing to ±2 kcal/mol for M102K. All entries represent data for folded T4 lysozymes that have the same numbers of buried or integral water molecules. Reversibility of thermal unfolding was judged by restoration of CD signal upon cooling and found to be in excess of 95%.

Acknowledgments

We thank Drs. Enoch Baldwin and Jon Wray for advice in mutagenesis and protein purification, and Drs. Larry Weaver and Dale Tronrud for help with X-ray data collection and refinement procedures. The work was supported in part by an NIH Postdoctoral Fellowship to L.A.L. (F32 CA65088) and a grant to B.W.M. (GM21967).

References

Alber T, Dao-pin S, Nye JA, Muchmore DC, Matthews BW. 1987. Temperature-sensitive mutations of bacteriophage T4 lysozyme occur at sites with low mobility and low solvent accessibility in the folded protein. *Biochemistry 26*:3754–3758.

Alber T, Matthews BW. 1987. Structure and thermal stability of phage T4 lysozyme. *Methods Enzymol 154*:511–533.

Creighton TE. 1992. *Protein folding*. New York: W.H. Freeman and Co.

Connolly ML. 1983. Solvent-accessible surfaces of proteins and nucleic acids. *Science 221*:709–713.

Dao-pin S, Anderson DE, Baase WA, Dahlquist FW, Matthews BW. 1991. The structural and thermodynamic consequences of burying a charged residue within the hydrophobic core of T4 lysozyme. *Biochemistry 30*:11521–11529.

Eriksson AE, Baase WA, Zhang X-J, Heinz DW, Blaber M, Baldwin EP, Matthews BW. 1992. The response of a protein structure to cavity-creating mutations and its relationship to the hydrophobic effect. *Science 255*:178–183.

Eriksson AE, Baase WA, Matthews BW. 1993. Similar hydrophobic replacements of Leu 99 and Phe 153 within the core of T4 lysozyme have different structural and thermodynamic consequences. *J Mol Biol 229*:747–769.

Estell DA, Graycar TP, Wells JA. 1985. Engineering an enzyme by site-directed mutagenesis to be resistant to chemical oxidation. *J Biol Chem 260*:6518–6521.

Faber HR, Matthews BW. 1990. A mutant T4 lysozyme displays five different crystal conformations. *Nature 348*:263–266.

Fauchére J-L, Pliška V. 1983. Hydrophobic parameters π of amino acid side-chains form the partitioning of N-acetyl-amino-acid amides. *Eur J Med Chem 18*:369–375.

Gassner NC, Baase WA, Matthews BW. 1996. A test of the "jigsaw puzzle" model for protein folding by multiple methionine substitutions within the core of T4 lysozyme. *Proc Natl Acad Sci USA 93*:12155–12158.

Gassner NC, Baase WA, Lindstrom JD, Shoichet BK, Matthews BW. 1997. Isolation and characterization of multiple-methionine mutants of T4 lysozyme with simplified cores. In: Marshak D, ed. Techniques in protein chemistry VIII. New York: Academic Press. pp 851–863.

Hamlin R. 1985. Multiwire area X-ray diffractometers. *Methods Enzymol 114*:416–452.

Hurley JH, Baase WA, Matthews BW. 1992. Design and structural analysis of alternative hydrophobic core packing arrangements in bacteriophage T4 lysozyme. *J Mol Biol 224*:1143–1159.

Kunkel TA, Roberts JD, Zakour RA. 1987. Rapid and efficient site-specific mutagenesis without phenotypic selection. *Methods Enzymol 154*:367–382.

Kuroki R, Weaver LH, Matthews BW. 1993. A covalent enzyme-substrate intermediate with saccharide distortion in a mutant T4 lysozyme. *Science 262*:2030–2033.

Matsumura M, Matthews BW. 1989. Control of enzyme activity by an engineered disulfide bond. *Science 243*:792–794.

Matthews BW. 1993. Structural and genetic analysis of protein stability. *Annu Rev Biochem 62*:139–160.

Muchmore DC, McIntosh LP, Russell CB, Anderson DE, Dahlquist FW. 1989. Expression and ^{15}N labelling of proteins for proton and nitrogen-15 NMR. *Methods Enzymol 177*:44–73.

Owen JE, Schultz DW, Taylor A, Smith GR. 1983. Nucleotide sequence of the lysozyme gene of bacteriophage T4: Analysis of mutations involving repeated sequences. *J Mol Biol 165*:229–248.

Pantoliano MW, Whitlow M, Wood JF, Dodd SW, Hardman KD, Rollence ML, Bryan PN. 1989. Large increases in general stability for subtilisin bpn' through incremental changes in the free energy of unfolding. *Biochemistry 28*:7205–7213.

Poteete AR, Dao-pin S, Nicholson H, Matthews BW. 1991. Second-site revertants of an inactive T4 lysozyme mutant restore activity structuring the active site cleft. *Biochemistry 30*:1425–1432.

Spencer DS, Stites WE. 1996. The M32L substitution of Staphylococcal nuclease: Disagreement between theoretical prediction and experimental protein stability. *J Mol Biol 257*:497–499.

Tronrud DE, Ten Eyck LF, Matthews BW. 1987. An efficient general-purpose least-squares refinement program for macromolecular structures. *Acta Crystallogr A43*:489–503.

Yamaotsu N, Moriguchi I, Hirono S. 1993. Estimation of stabilities of staphylococcal nuclease mutants (Met^{32} → Ala and Met^{32} → Leu) using molecular dynamics/free energy perturbation. *Biochim Biophys Acta 1203*:243–250.

Zhang X-J, Baase WA, Shoichet BK, Wilson KP, Matthews BW. 1995. Enhancement of protein stability by the combination of point mutations in T4 lysozyme is additive. *Protein Eng 8*:1017–1022.

Zhang X-J, Matthews BW. 1995. EDPDB: A multi-functional tool for protein structure analysis. *J Appl Crystallogr 28*:624–630.